Iranian Polymer Journal (2019) 28:39–49
https://doi.org/10.1007/s13726-018-0677-7

ORIGINAL RESEARCH

Self-assembly and drug release control of dual-responsive copolymers based on oligo(ethylene glycol)methyl ether methacrylate and spiropyran

Zhouxiaoshuang Yang[1] · Hu Zou[1] · Hui Liu[1,2] · Wenshuang Xu[1] · Lulu Zhang[1]

Received: 2 July 2018 / Accepted: 26 November 2018 / Published online: 30 November 2018
© Iran Polymer and Petrochemical Institute 2018

Abstract

To compare the synthesis and drug release of random and block copolymers, random and block copolymerizations of oligo(ethylene glycol)methyl ether methacrylate (OEGMA) and 1′-(2-methacryloxyethyl)-3′,3′-dimethyl-6-nitrospiro-(2H-1-benzopyran-2,2′-indoline) (SPMA) were carried out by atom transfer radical polymerization. The ^{1}H NMR and GPC results indicated the targeted random and block copolymers were successfully synthesized. Critical micelle concentrations of random and block copolymers were determined as 0.0178 mg/mL and 0.0265 mg/mL, and the micelle aggregation numbers of the random and block copolymers were calculated as approximately 17 and 13, respectively, indicating that more molecular chains were required to form a stable polymeric micelle for a random than its block copolymer. A lower critical solution temperature of 37 °C, the human body temperature, was obtained for two copolymer samples, suggesting that they might have potential application in the biomedical field. During the self-assembly, the morphology of block copolymer micelles was more regular than that of random copolymer, and both copolymers exhibited the exchange of hydrophilic and hydrophobic segments called as "Schizophrenic" behavior under UV light irradiation at 50 °C. With doxorubicin as a model molecule in drug release control, heating and ultraviolet light irradiation could accelerate the drug release process to some extent, indicating the potential application of the resulting random and block copolymers in drug release and bioengineering.

Keywords Amphiphilic copolymer · Stimuli-responsive · Self-assembly · Drug release control · Doxorubicin

Introduction

Stimuli-responsive materials have attracted more and more interest in the past few decades due to their potential application in catalyst, nanoreactor, biosensor, tissue engineering, and drug release control [1–3]. Among these smart materials, stimuli-responsive amphiphilic copolymers have been very much investigated because they can form regular aggregates by the self-assembly process [4–6]. These copolymers gather together through hydrophobic forces and tend to form aggregates with certain morphology. All micelles, vesicles, and bars can be obtained under specific conditions, which are mainly dependent on the critical accumulation parameters in the self-assembly process [7–9]. Block and random copolymers are two classes of copolymers, and each has its own advantages. In contrast to random copolymers, the synthesis process of block copolymers is usually more complex and time consuming, but their self-assembly morphology is normally more regular and clear.

There exists a poor hydrogen bonding interaction between thermo-responsive polymers and water molecules, by making polymers to exhibit a lower critical solution temperature (LCST) in aqueous solution [10–12]. Aqueous solution becomes more hydrophobic with the increase in temperature and becomes turbid when the temperature is higher than its LCST. Poly(*N*-isopropylacrylamide) (PNIPAm), a popular thermo-responsive polymer, due to its simple structure and

Electronic supplementary material The online version of this article (https://doi.org/10.1007/s13726-018-0677-7) contains supplementary material, which is available to authorized users.

✉ Hui Liu
liuhui@csu.edu.cn

[1] College of Chemistry and Chemical Engineering, Central South University, Changsha 410083, Hunan, People's Republic of China

[2] Hunan Provincial Key Laboratory of Efficient and Clean Utilization of Manganese Resources, Central South University, Changsha 410083, Hunan, People's Republic of China

low price, has been studied extensively elsewhere [13–15]. Tang et al. [16] synthesized a thermo/pH dual-responsive hydrophilic brush-coil copolymer PNIPAM-*b*-(PGMA-*g*-PLGA), and the self-assembly experiments were also carried out. Their work showed that the resulting responsive copolymers had potential application in the biomedical materials. However, biocompatibility is an important and desirable factor in the biomedicine domain [1, 17]. In recent years, a new series of poly-oligo(ethylene glycol) methyl ether methacrylates (POEGMAs), which are highly nontoxic and biocompatible, displays a lot of advantages in drug release control [18, 19]. Skandalis and Pispas [20] synthesized PDMAEMA-*b*-PLMA-*b*-POEGMA triblock terpolymers through RAFT polymerization, and studied their self-assembly behaviors under different conditions. Furthermore, Lutz's [17] work showed that the hydrophilic–hydrophobic transformation of $PMEO_3MA$ (one class of POEGMA) was rather sharp, and its LCST range was relatively narrower than that of PNIPAm. In addition, the cooling curve of $PMEO_3MA$ was almost the same as its heating curve, whereas there was an obvious lag between the cooling and heating curves for PNIPAm. All POEGMA advantages have been of interest for many researchers in recent years.

At the same time, photo-responsive materials are developed rapidly since the wavelength and intensity of light are easily controlled [21–23]. Families of photochromic compounds commonly used in the polymeric systems include azobenzenes [24, 25], spiropyrans [26, 27], spirooxazines [28], diarylethenes [29], and fulgides [30]. Lodge et al. [31] synthesized a series of photo-responsive copolymers P(AzoMA-*r*-NIPAm), and they found a block copolymer which could be reversibly transferred into a micelle in an ionic liquid under light illumination. Quick response to external stimuli is a strong demand for photo-responsive polymers therefore, among them spiropyrans have been extensively studied because of their quick response rate and reversible isomerization. Furthermore, spiropyran compounds have various potential application domains such as cell labeling [32–34], selective ion detecting [35], drug delivery [36–38], and so on.

In our previous work, we successfully synthesized photo- and thermo-dual-responsive amphiphilic random copolymer P(MEO_3MA-*co*-SPMA), and used its self-assembly for release control with doxorubicin (DOX) as the model drug [39]. Based on a previous work, we think it would be better to compare the drug release efficiency between random and block copolymers with the same organic monomers. Therefore, in the present work, we synthesized two classes of copolymers including: random copolymer P(MEO_2MA-*co*-MEO_3MA-*co*-SPMA) and block copolymer P(MEO_2MA-*co*-MEO_3MA)-*b*-PSPMA by atom transfer radical polymerization (ATRP). The LCSTs of these resulting copolymers were mainly regulated by altering feed molar ratio of MEO_2MA/MEO_3MA, and the copolymers were used for drug release experiments of DOX. To the best of our knowledge, this is the first time that the synthesis and drug release of random and block copolymers of OEGMA and spiropyran derivatives are studied and compared with each other.

Experimental

Materials

Di(ethylene glycol)methyl ether methacrylate (MEO_2MA, Aldrich, 95%) and tri(ethylene glycol)methyl ether methacrylate (MEO_3MA, Aldrich, 94%) were passed through a column of basic alumina to remove inhibitors before use. The photo-responsive monomer, 1′-(2-methacryloxyethyl)-3′,3′-dimethyl-6-nitrospiro-(2H-1-benzopyran-2,2′-indoline) (SPMA), was prepared by the previously reported method [39]. Copper(I) bromide (CuBr, 99%, Aladdin) as the catalyst was purified by stirring in boiling glacial acetic acid for 10 min, and then washed several times with ethanol and diethyl ether. Doxorubicin (DOX) as the model drug was obtained by the reaction of doxorubicin hydrochloride (DOX·HCl, 95%, TCI) and triethylamine (TEA, 98%, TCI). *N,N,N′,N″,N‴*-Pentamethyldiethylenetriamine (PMDETA, 98%, TCI) as the ligand, ethyl 2-bromoisobutyrate (EBiB, 98%, TCI) as the initiator, dichloromethane (DCM, 99%, J&K), tetraethyl orthosilicate (TEOS, 99.5%), ethanol (98%), tetrahydrofuran (THF, 99%), triethylamine (TEA, 99%), (3-aminopropyl)-triethoxy-silane (APTES, 99.6%, J&K), and *n*-hexane (98%) were all used as received.

Characterization

Structure and composition of the resulting random and block copolymers were characterized by a Bruker (400 MHz AVANCE III) NMR spectrometer, with $CDCl_3$ as the solvent. Molecular weights (M_n) and polydispersity (M_w/M_n) of the copolymers were determined by a gel permeation chromatography (GPC) instrument (Waters 1515). THF was used as the mobile phase at a flow rate of 1 mL/min with standard polystyrene as the calibration curve.

Critical micelle concentrations (CMCs) of the random and block copolymeric micelles were determined by the fluorescence emission spectra of pyrene on an F-4600 fluorescence instrument. Micelle aggregation number (N_{agg}) was measured using pyrene as the fluorescence probe in the presence of benzophenone as the quencher at 25 °C. Measurement of the accumulation release of doxorubicin was conducted on a UV-2600/2700 ultraviolet and visible spectrophotometer with the power of 12 W. A lower critical solution temperature (LCST) was also obtained.

Self-assembly morphology of copolymers was observed on a Titan G2 60–300 transmission electron microscope (TEM) at an acceleration voltage of 300 kV. TEM sample was produced by evaporating 10 μL self-assembly solution on copper grids coated with thin films of Formvar and carbon at room temperature. Particle sizes of self-assembled nanoparticles were measured by dynamic light scattering (DLS) at room temperature (25 °C) by a Malvern Zetasizer Nano Men3600. Specifically, determination of particle size for MC micelles was carried out in almost dark conditions to avoid the possible isomerization from MC to SP form under visible light.

Synthesis and self-assembly of copolymers

Synthesis of random copolymer P(MEO_2MA-*co*-MEO_3MA)

MEO_2MA (0.685 mL, 3.5 mmol), MEO_3MA (0.845 mL, 3.5 mmol), CuBr (6.8 mg, 0.07 mmol), ethanol (5 mL), and EBiB (10 μL, 0.07 mmol) were added into a 25 mL Schlenk tube. Then, the tube was put under high purity nitrogen atmosphere for 0.5 h to remove oxygen. Later, PMDETA (106 μL, 0.07 mmol) was carefully injected into the tube with a microliter syringe. The Schlenk tube was placed in an oil bath at 60 °C for 20 h with magnetic stirring. The polymerization was stopped by exposing the tube to air. The raw compound was diluted with 5 mL ethanol and then passed through a neutral alumina column to remove the residual copper catalyst. Finally, *n*-hexane as the precipitant was introduced to obtain the targeted product. The resulting residue was dried under vacuum for 24 h to evaporate the remained *n*-hexane. By regulating feed molar ratio percentage of MEO_3MA, 11 samples were successfully obtained, and Scheme 1a shows the preparation route of P(MEO_2MA-*co*-MEO_3MA).

Synthesis of random copolymer P(MEO_2MA-*co*-MEO_3MA-*co*-SPMA)

MEO_2MA (0.820 mL, 4.2 mmol), MEO_3MA (0.675 mL, 2.8 mmol), SPMA (54 mg, 0.13 mmol), CuBr (6.8 mg, 0.07 mmol), ethanol (5 mL), and EBiB (10 μL, 0.07 mmol) were added into a 25 mL Schlenk tube. The main synthesis process was conducted as the procedure for P(MEO_2MA-*co*-MEO_3MA) as depicted in Scheme 1b. As shown in Table 1, the feed molar ratios of MEO_2MA:MEO_3MA were 60:40, 55:45, 50:50, and 30:70, and the resulting random copolymers were labeled as *R*1, *R*2, *R*3, and *R*4, respectively.

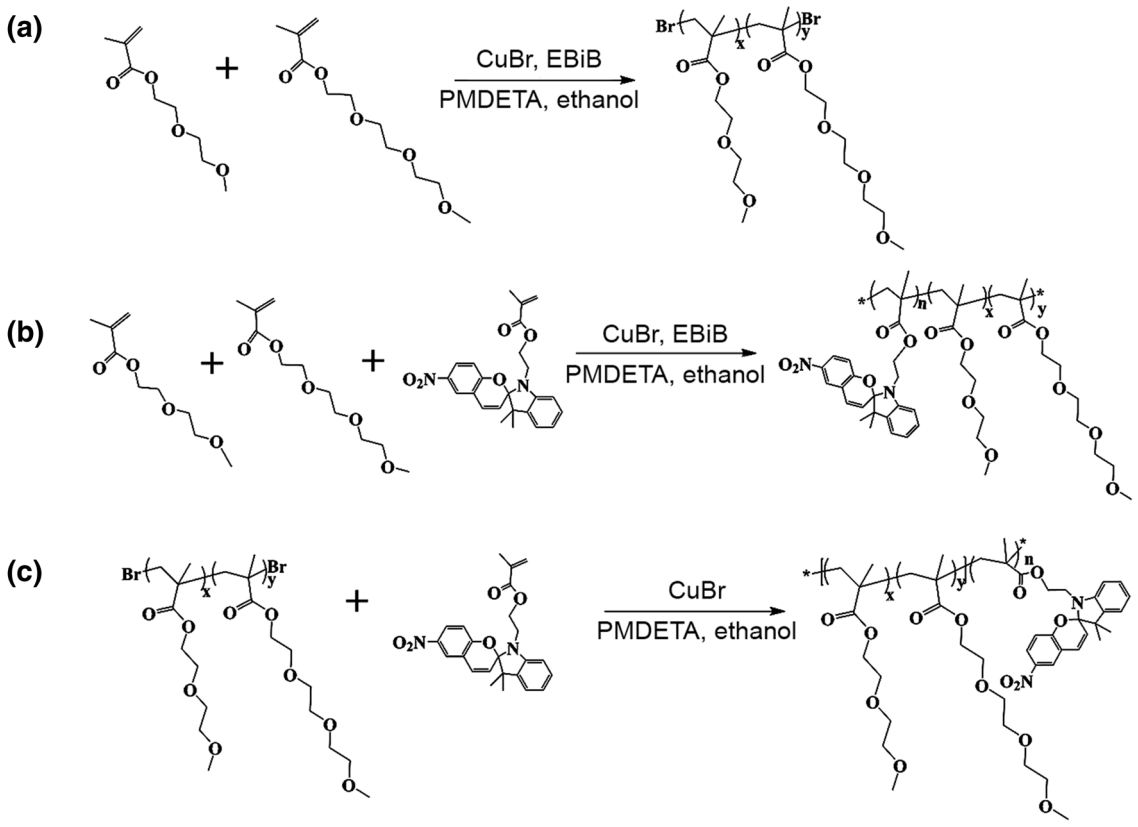

Scheme 1 Synthesis process of **a** P(MEO_2MA-*co*-MEO_3MA) **b** P(MEO_2MA-*co*-MEO_3MA-*co*-SPMA), and **c** P(MEO_2MA-*co*-MEO_3MA)-*b*-PSPMA

Table 1 Structure unit ratio, GPC, and LCST details of random and block copolymers

Polymers	Num.	Feed molar ratio (MEO_2MA:MEO_3MA:SPMA)	Structure unit ratio (MEO_2MA:MEO_3MA:SPMA)	M_n (g/mol)	M_W (g/mol)	PDI	LCST (°C)
P(MEO_2MA-*co*-MEO_3MA-*co*-SPMA)	*R*1	59:39:2	45:52:3	19,162	30,939	1.58	27
	*R*2	54:44:2	38:58:4	14,914	22,534	1.51	30
	*R*3	49:49:2	33:64:3	21,598	40,548	1.88	31
	*R*4	29:69:2	13:84:3	21,208	35,352	1.67	37
P(MEO_2MA-*co*-MEO_3MA)-*b*-PSPMA	*X*1	49:49:2	45:51:4	25,934	40,048	1.54	35
	*X*2	39:59:2	35:64:1	32,753	62,798	1.92	37
	*X*3	29:69:2	30:68:2	30,029	47,307	1.58	38

Synthesis of block copolymer P(MEO_2MA-*co*-MEO_3MA)-*b*-PSPMA

General synthesis procedure of block copolymer P(MEO_2MA-*co*-MEO_3MA)-*b*-PSPMA contained two steps. The first step involved the synthesis of P(MEO_2MA-*co*-MEO_3MA)-Br as a ATRP macroinitiator. It was obtained by adding MEO_2MA (0.545 mL, 2.8 mmol), MEO_3MA (1.015 mL, 4.2 mmol), CuBr (9.8 mg, 0.07 mmol), ethanol (5 mL), EBiB (10 µL, 0.07 mmol), and PMDETA (106 µL, 0.07 mmol) into a Schlenk tube under protection of high purity nitrogen as described above. Three macroinitiators were synthesized in which feed molar ratios of MEO_2MA:MEO_3MA were 30:70, 40:60, and 50:50, respectively. The second step was synthesis of block copolymer as follows: P(MEO_2MA-*co*-MEO_3MA)-Br (0.278 g, ~0.024 mmol), SPMA (54 mg, 0.13 mmol), CuBr (1.8 mg, 0.018 mmol), ethanol (1 mL), and PMDETA (50 µL, 0.033 mmol) were added into a degassed Schlenk tube. All reaction conditions and post-process of two steps were the same as those described above. The synthetic process of P(MEO_2MA-*co*-MEO_3MA)-*b*-PSPMA can be seen in Scheme 1c. The feed molar ratios of MEO_2MA:MEO_3MA were 50:50, 40:60, and 30:70, and the resulting block copolymers were labeled as *X*1, *X*2, and *X*3, respectively.

Self-assembly process of random copolymers and block copolymers

Self-assembly processes were carried out according to our previous work [39].

Drug encapsulation and release of doxorubicin for the self-assembly

The amount of 27 mg of each sample (sample *R*4 for random copolymer, and sample *X*2 for block copolymer) and 3.7 mg of DOX were dissolved in 7 mL DMF. Then, DOX was encapsulated by gradually injecting 7 mL deionized water with a dropping speed of 1.5 mL/h. After injection, the mixture was dialyzed for 3 days to remove extra DMF and unloaded DOX. Finally, the system was diluted to 1 mL/h. The quantity of loaded DOX was determined by the UV–Vis absorption spectrum at the wavelength of 480 nm by deducting the quantity of unloaded DOX in the obtained supernatant from the quantity of initial feeding DOX. Drug loading efficiency (DLE) was calculated according to Eq. 1 as follows:

$$\text{DLE (wt\%)} = \frac{\text{weight of feeding drug} - \text{weight of unloaded drug}}{\text{weight of feeding drug}} \times 100\%. \quad (1)$$

Drug release process was conducted by continuous measurement of daily sate of drug carrier under different conditions for 24 h. The amount of 2 mL of self-assembled carrier with DOX was added into a dialysis bag and then it was immersed into 8 mL of a phosphate buffer solution (PBS, 0.01M, pH 7.4). Then, 3 mL dialysis solution was collected, and 3 mL fresh PBS solution was added at the same time to keep the total volume constant. The mass of DOX for its accumulative release was calculated according to the following equation [40, 41]:

$$\text{DOX release (mg)} = Ve \sum_{1}^{n-1} c_i + c_n V_0 \quad (2)$$

where *DOX release* is the mass of accumulative release for DOX, *Ve* is the volume of collected solution during the controlled release process, c_i is the concentration of dialysis fluid, *n* is the sample-extracting times, and V_0 is the total volume.

Results and discussion

Structure characterization of random and block copolymers

Random and block copolymers were all synthesized by ATRP, and their ^{1}H NMR spectra are shown in Fig. 1.

According to the characteristic peaks of the curve (a) in Fig. 1, it can be concluded that P(MEO_2MA-*co*-MEO_3MA) is successfully synthesized. The structure unit molar ratio of P(MEO_2MA-*co*-MEO_3MA) was calculated based on integral area ratio between the peaks at δ_1 3.74, δ_2 3.65, δ_3 3.57 and δ_4 3.39.

The LCSTs of all P(MEO_2MA-*co*-MEO_3MA) samples are listed in Table S1 in the Supplementary Material. The LCSTs of homopolymers PMEO_2MA and PMEO_3MA are 27 °C and 52 °C, respectively, which are in accordance with the previous publications [18, 42]. The relationship between LCST of P(MEO_2MA-*co*-MEO_3MA) and feed molar ratio of MEO_2MA/MEO_3MA is shown in Fig. 2. As can be observed, the LCST of random copolymer P(MEO_2MA-*co*-MEO_3MA) gradually increases linearly with the rising feed molar percentage of MEO_3MA. It is suggested that we can obtain the copolymers with the desirable LSCT in the range from 27 °C to 52 °C by regulating the feed molar ratio of MEO_2MA/MEO_3MA. These adjustable LCST values in Fig. 2 lay an important theoretical and practical foundation for the further synthesis of the triple copolymers.

From the curve (b) in Fig. 1, obvious characteristic peaks of MEO_2MA/MEO_3MA unit and characteristic peaks of SPMA are observed, implying the successful synthesis of random copolymer P(MEO_2MA-*co*-MEO_3MA-*co*-SPMA) (sample *R*2). The peaks at δ_1 3.74, δ_2 3.65, δ_3 3.57, δ_4 3.39, δ_5 8.01, and δ_6 7.96 were employed to calculate the structural unit ratio of P(MEO_2MA-*co*-MEO_3MA-*co*-SPMA). By adjusting feed molar ratio of MEO_2MA/MEO_3MA, four samples with different structural unit ratios were obtained. The ^{1}H NMR spectra of other three samples (*R*1, *R*3, and *R*4) are presented in the Supplementary Material (Figs. S1–S3). More details of these random copolymers and their molecule weights are listed in Table 1.

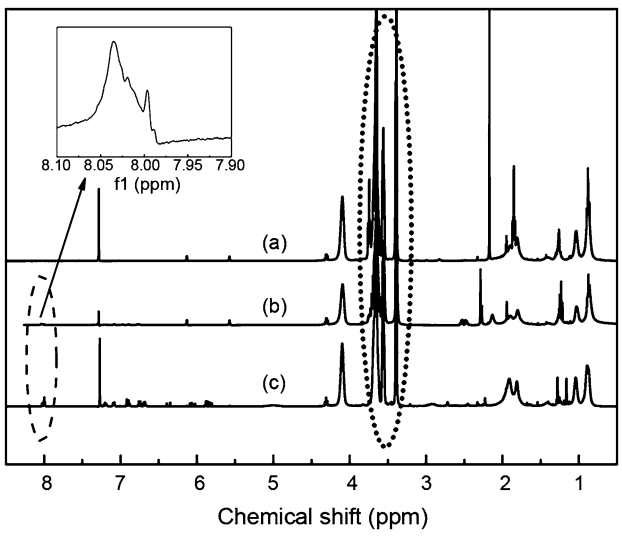

Fig. 1 ^{1}H NMR spectra of **a** P(MEO_2MA-*co*-MEO_3MA), **b** P(MEO_2MA-*co*-MEO_3MA-*co*-SPMA) (*R2*), and **c** P(MEO_2MA-*co*-MEO_3MA)-*b*-PSPMA (*X1*)

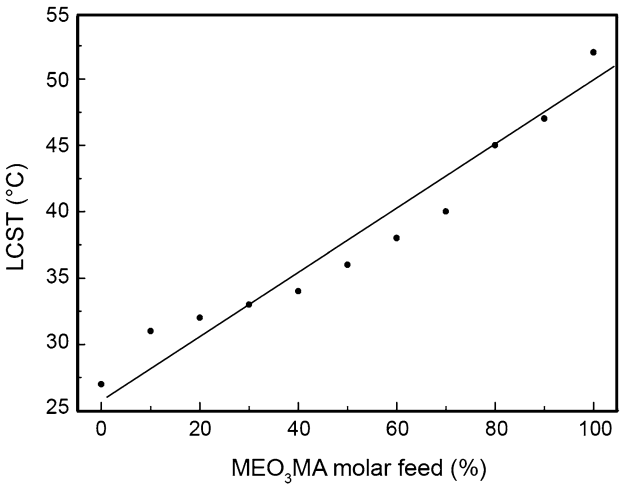

Fig. 2 Linear relationship between LCST of P(MEO_2MA-*co*-MEO_3MA) and feed molar ratio of MEO_2MA/MEO_3MA. All samples were measured at a concentration of 3 mg/mL

Block copolymer P(MEO_2MA-*co*-MEO_3MA)-*b*-PSPMA was synthesized through a two-step ATRP, and P(MEO_2MA-*co*-MEO_3MA)-Br was used as the macromolecular initiator in the latter reaction. In the ^{1}H NMR spectrum of P(MEO_2MA-*co*-MEO_3MA)-*b*-PSPMA (sample *X*1) shown in the curve (c) in Fig. 1, characteristic peaks similar to those observed in the curve (b) can be seen. The ^{1}H NMR spectra of *X*2 and *X*3 are shown in Supplementary Material (Figs. S4–S5). Their molecular weights and distributions are also presented in Table 1.

In addition, critical micelle concentration (CMC) of the random and block copolymers was determined by the fluorescence spectra of pyrene, and the results are shown in Figs. S6 and S7, respectively (in Supplementary Material). As can be seen, CMCs of the random and block copolymers are 0.0178 mg/mL and 0.0265 mg/mL, respectively, and it is possibly attributed to the shorter SPMA polymeric chains in the block copolymer (sample *X*2) compared to the chains in random copolymer (sample *R*4).

Also, the micelle aggregation numbers of random P(MEO_2MA-*co*-MEO_3MA-*co*-SPMA) (sample *R*4) and block P(MEO_2MA-*co*-MEO_3MA)-*b*-PSPMA (sample *X*2) copolymers were measured at 25 °C, and the results are listed in Fig. S8 in Supplementary Material (in Fig. S8, I_0 and I in *Y*-axis are the fluorescence intensities before and after the addition of benzophenone as the quencher, respectively, and C_Q in *X*-axis refers to quencher concentration). As determined from the slope of the fitting straight line in Fig. S8 (in Supplementary Material), the micellar aggregation numbers of the random and block

copolymeric were found to be approximately 17 and 13, respectively. More molecular chains were required to form a stable polymeric micelle for random sample *R*4 than that for block sample *X*2, attributed by more irregular molecular structure of random copolymer chains.

Thermo- and photo-dual-responsive behavior of copolymers

Photo-responsive behaviors of copolymers

Photo-responsive behavior of the random copolymer P(MEO_2MA-*co*-MEO_3MA-*co*-SPMA) was revealed by UV–Vis absorption spectrophotometry, and the results are shown in Fig. 3a, b. The random copolymer (sample *R*1) was dissolved in deionized water (3 mg/mL) with different ultraviolet (UV) light (365 nm, 12 W) irradiation time intervals. As shown in Fig. 3a, b, the relative absorbance of SPMA gradually varies, and attains its maximum peak at the wavelength of 550 nm. Spiropyran-based polymer unit consists of two orthogonal aromatic rings with a sp^3 hybridization carbon atom, and this structure can realize a reversible transformation between hydrophobic spiropyran (SP) and hydrophilic merocyanine (MC). Therefore, the absorbance intensity at 550 nm increases with the UV light irradiation time and decreases with the visible light irradiation time. The outcomes in Fig. 3a, b suggest that the random copolymer P(MEO_2MA-*co*-MEO_3MA-*co*-SPMA) has a strong reversible photosensitive behavior.

Photo-responsive behavior of the block copolymer P(MEO_2MA-*co*-MEO_3MA)-*b*-PSPMA was also characterized by UV–Vis absorption spectrophotometry, and the results are demonstrated in Fig. 3c, d. It can be seen that the maximum absorption wavelength of the block copolymer

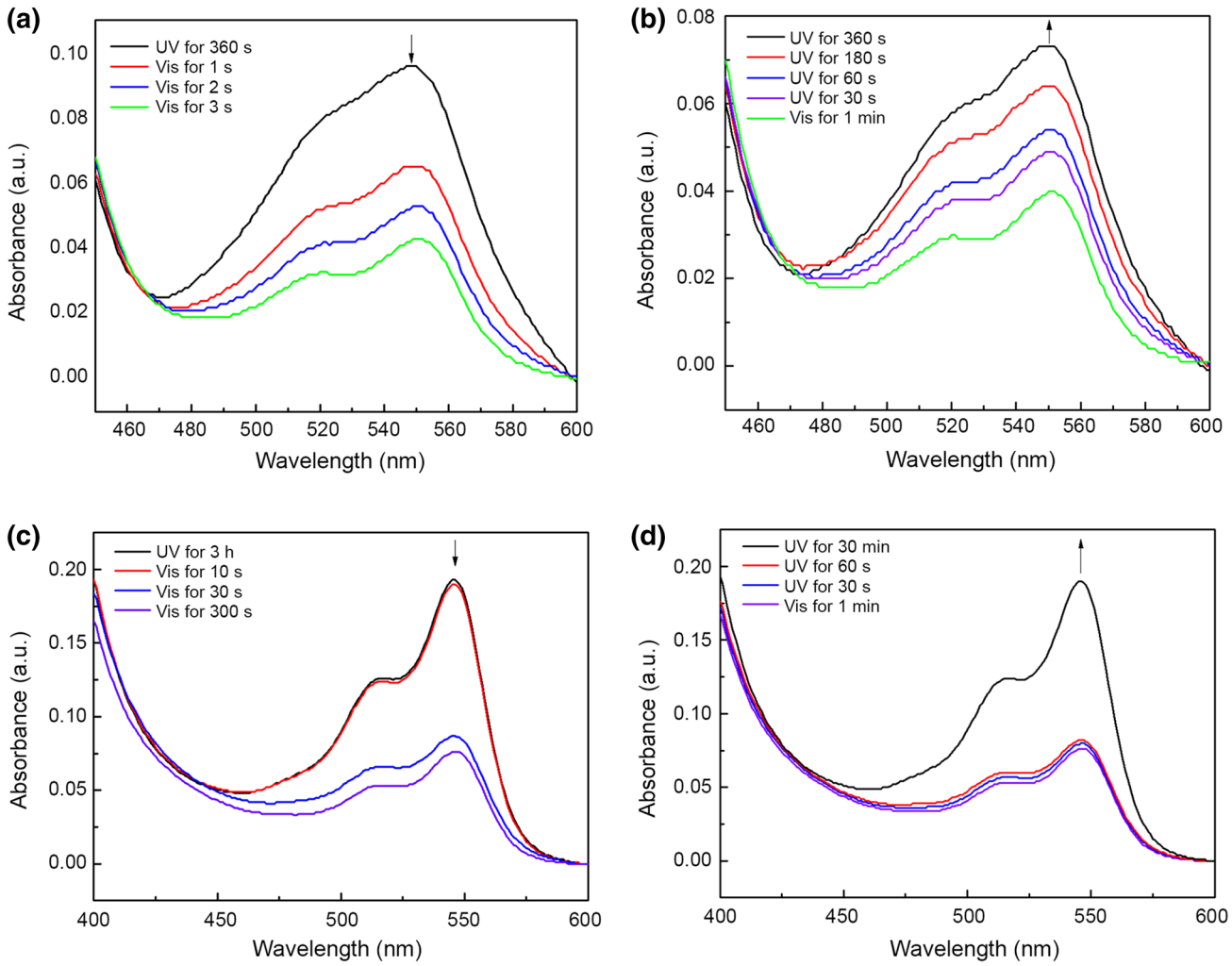

Fig. 3 UV–Vis absorption spectra of triple copolymers at different light irradiations: **a** visible light induced-ring closing of P(MEO_2MA-*co*-MEO_3MA-*co*-SPMA); **b** UV light induced-ring opening of P(MEO_2MA-*co*-MEO_3MA-*co*-SPMA); **c** visible light induced-ring closing of P(MEO_2MA-*co*-MEO_3MA)-*b*-PSPMA; **d** UV light induced-ring opening of P(MEO_2MA-*co*-MEO_3MA)-*b*-PSPMA

reaches a strong peak at about 545 nm, which is slightly blue shifted from that of random copolymer P(MEO_2MA-*co*-MEO_3MA-*co*-SPMA). Certainly, blue shift, a shift of MC peak to shorter wavelengths, usually occurs upon increasing the polarity, and this negative solvatochromism is related to the stabilization of the planar zwitterionic MC form [43, 44]. It also implies that the type of polymer has an effect on the maximum absorption wavelength of spiropyran segment to some extent. Notably, the closing loop of P(MEO_2MA-*co*-MEO_3MA)-*b*-PSPMA in Fig. 3c takes longer visible light irradiation time than that of P(MEO_2MA-*co*-MEO_3MA-*co*-SPMA) in Fig. 3a, which is due to the difference in the power of visible lamps (300 W in former experiments and 12 W in the present and next sections). The absorbance spectrum of P(MEO_2MA-*co*-MEO_3MA)-*b*-PSPMA from Fig. 3c, d also indicates that the block copolymer prepared by ATRP is photosensitive.

Thermo-responsive behavior of copolymers

LCSTs of the random copolymer P(MEO_2MA-*co*-MEO_3MA-*co*-SPMA) and block copolymer P(MEO_2MA-*co*-MEO_3MA)-*b*-PSPMA were measured by transmittance experiments according to the midpoint of position with the maximum slope of straight line. As illustrated in Fig. 4a, b, all the LCST values of the random and block copolymers increase with the increase in feed molar ratio portion of MEO_3MA unit. In addition, the LCSTs of both samples *R*4 and *X2* are closer to human body temperature (37 °C), indicating that they may have potential applications in biomedical field. The details of LCSTs of the random and block copolymers are also listed in Table 1. It is suggested that the LCSTs of block polymers are a little higher than those of random copolymers, which can be explained by more regular molecular structure of the block copolymers. Moreover, this result is also in good agreement with the CMC results mentioned above.

Self-assembly of random and block copolymers

TEM micrographs of self-assembly aggregates for the random copolymer P(MEO_2MA-*co*-MEO_3MA-*co*-SPMA) and block copolymer P(MEO_2MA-*co*-MEO_3MA)-*b*-PSPMA are shown in Fig. 5. Samples *R*4 and *X*2 were selected and dissolved in THF to conduct self-assembling process with four types of stimulation. In general, both hydrophilic and hydrophobic portions are required for the construction of self-assembly, so in Fig. 5a, a′, we can see obvious spherical micelles at visible light irradiation at 20 °C. As we expected, spherical micelles in Fig. 5a′ seem much more regular than those in Fig. 5a, indicating that the self-assembly of block copolymer is better controlled than that of random copolymer.

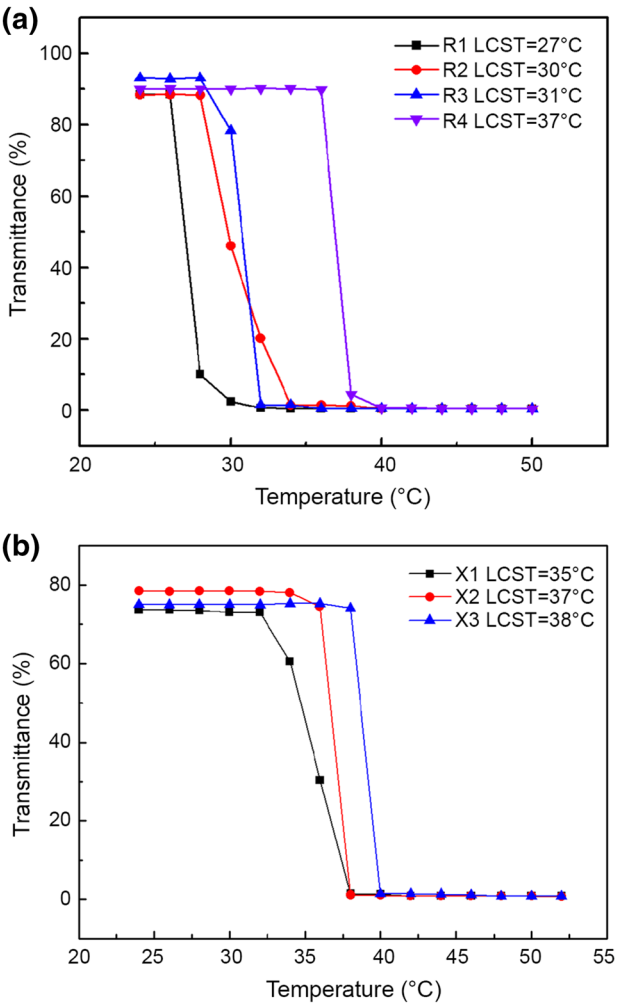

Fig. 4 Diagram of LCST values for triple copolymers with different feed molar ratios **a** P(MEO_2MA-*co*-MEO_3MA-*co*-SPMA) **b** P(MEO_2MA-*co*-MEO_3MA)-*b*-PSPMA. All samples were measured at a concentration of 3 mg/mL

Under UV light irradiation and at 50 °C, the micelles with core–shell structure are clearly observed in Fig. 5d, d′ due to the exchange of hydrophilic and hydrophobic segments in the copolymers as called "Schizophrenic" behavior in published literature [45–47]. However, only some free amorphous copolymeric segments can be seen in Fig. 5b, b′. This is because the hydrophobic SP segments are isomerized into hydrophilic MC unit at UV light irradiation and the OEGMA unit exhibits hydrophilic nature at 20 °C. In the contrary, when both segments in the molecular structure of copolymers are hydrophobic, we can still see some clear micelles at visible light irradiation and at 50 °C as shown in Fig. 5c, c′, possibly caused by the synergistic effect of two monomer units.

To compare micelle sizes with different self-assembling conditions, DLS experiments were also conducted in this

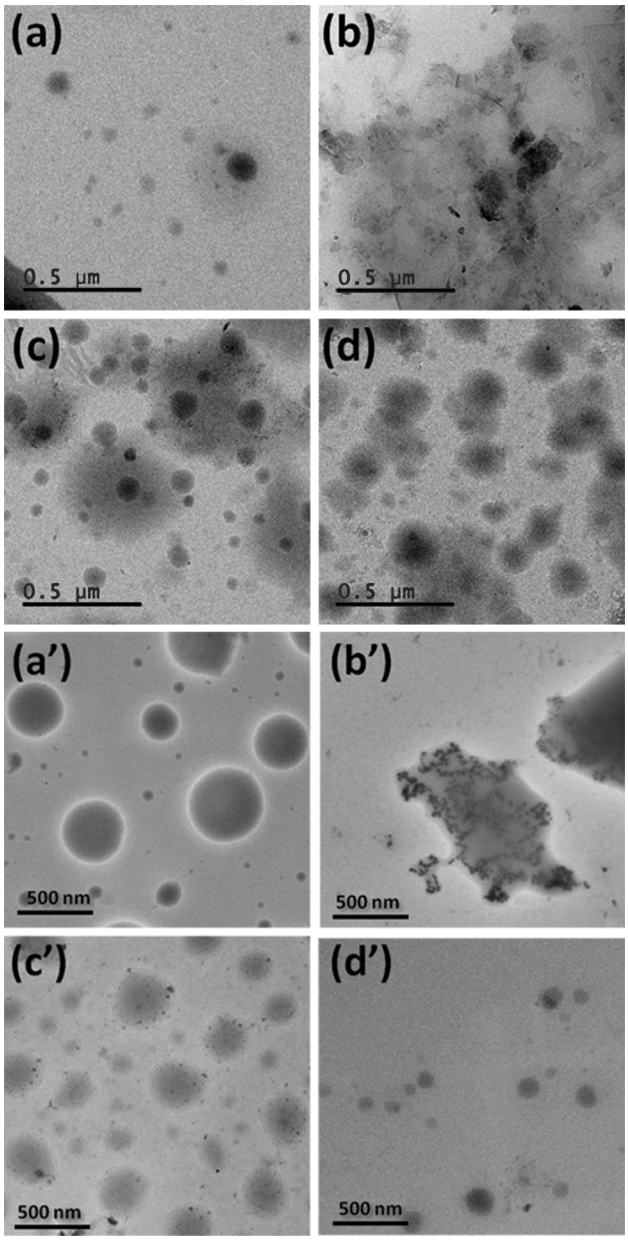

Fig. 5 TEM images of self-assemblies for P(MEO_2MA-*co*-MEO_3MA-*co*-SPMA) (*R*4): **a** visible light irradiation at 20 °C; **b** UV light irradiation at 20 °C; **c** visible light irradiation at 50 °C; **d** UV light irradiation at 50 °C. TEM images of self-assemblies for P(MEO_2MA-*co*-MEO_3MA)-*b*-PSPMA (*X*2): **a′** visible light irradiation at 20 °C; **c′** UV light irradiation at 20 °C; **b′** visible light irradiation at 50 °C; **d′** UV light irradiation at 50 °C

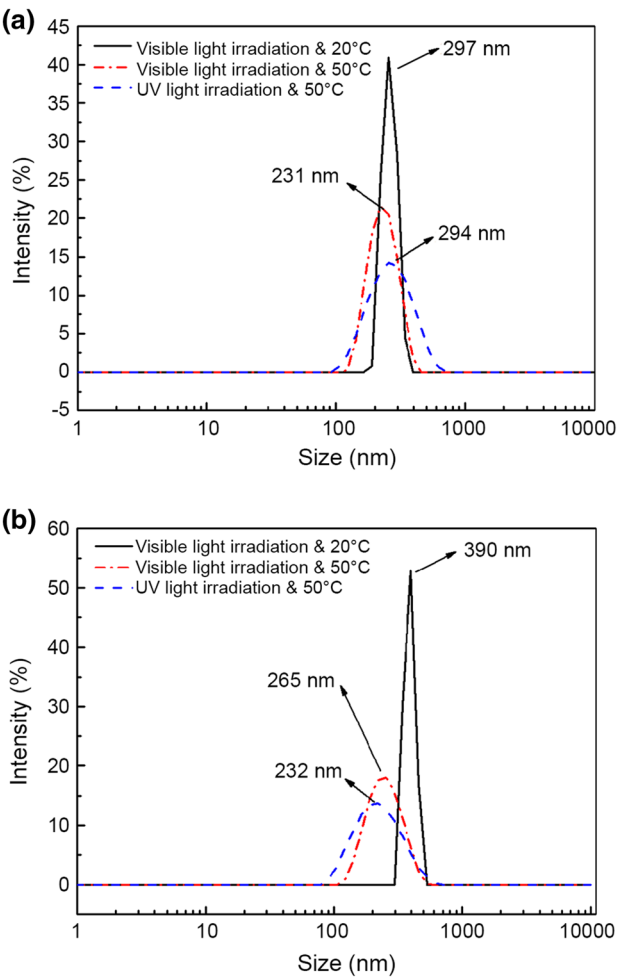

Fig. 6 Size distribution for self-assemblies of **a** P(MEO_2MA-*co*-MEO_3MA-*co*-SPMA) and **b** P(MEO_2MA-*co*-MEO_3MA)-*b*-PSPMA

work, and the results are displayed in Fig. 6. As can be found, the biggest micelle sizes of the random copolymer P(MEO_2MA-*co*-MEO_3MA-*co*-SPMA) and block copolymer P(MEO_2MA-*co*-MEO_3MA)-*b*-PSPMA are 297 nm and 390 nm, respectively, under visible light irradiation and at 20 °C. With increasing self-assembly temperature, OEGMA segments in the copolymers start to shrink, leading to smaller micellar size. When OEGMA and SPMA exchange their hydrophilic–hydrophobic properties under UV light irradiation and at 50 °C, their micelle sizes are still smaller than before exchanging process. It can be attributed to the fact that less SPMA portion in the copolymer chains becomes the shell for micelles in this case. In addition, the particle sizes also depend on the change in LCSTs of random and block copolymers to some extent. Nevertheless, LCSTs of both samples *R4* and *X*2 are approximately 37 °C as shown in Fig. 4, so the effect of LCST on particle sizes may be small in this situation.

DOX release control of copolymers self-assembly

Due to the hydrophobic interactive force, amphiphilic copolymers could be self-assembled into nanomicelles and used to encapsulate hydrophobic drug. Drug loading and release control experiments of random P(MEO_2MA-*co*-MEO_3MA-*co*-SPMA) and block copolymers

P(MEO_2MA-*co*-MEO_3MA)-*b*-PSPMA were both carried out, and the schematic representation of drug loading and release is shown in Scheme 2. Samples *R*4 and *X*2 were chosen to load the hydrophobic doxorubicin (DOX) because of their specific LCST (37 °C) near to the human body temperature. Drug-loading efficiencies (DLE) of *R*4 and *X*2 were experimentally determined as 47.5% and 58.2%, respectively, showing the advantage of block copolymer (*X*2) during drug loading. Photo- and thermo-stimuli were used to induce hydrophilic–hydrophobic transformation of amphiphilic copolymers. Monitored by UV–Vis spectrophotometer, the accumulative drug release of self-assembly was quantitatively calculated by the standard curve of DOX as shown in Fig. S9 in Supplementary Material.

Since LCSTs of the random and block copolymers in the present work were located in the range of 27–38 °C, we assumed that the great change might be observed when the temperatures were lower and higher than LCSTs of the copolymers. Based on this, temperatures of 20 °C and 50 °C were chosen to induce the thermal responsive behaviors during the drug release.

The accumulative drug release for P(MEO_2MA-*co*-MEO_3MA-*co*-SPMA) self-assembly aggregates at different complex stimuli conditions is displayed in Fig. 7. With the prolonging dialysis time, an obvious increase of the accumulative drug release is observed, except under the condition of visible light irradiation at 20 °C. It is because the self-assembly maintains the hydrophilic/hydrophobic balance under the condition of visible light irradiation at 20 °C. Moreover, the amount of drug release of self-assembly under the same light irradiation situation is increased with elevating temperature from 20 to 50 °C. The reason why heating can dominate the drug release process (relative to UV light irradiation) is that there is much more OEGMA segments in the copolymeric chains than SPMA unit. Furthermore, drug release amount of self-assembly aggregates under visible light irradiation is lower than that of under UV light irradiation at the same temperature.

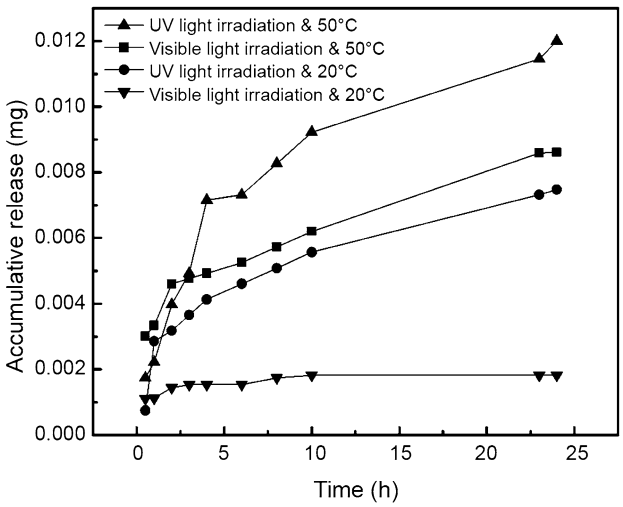

Fig. 7 Accumulative drug release for P(MEO_2MA-*co*-MEO_3MA-*co*-SPMA) self-assembly at different stimuli conditions

As we mentioned above, a molecular drug is usually encapsulated in the core during the self-assembly process under visible light irradiation at 20 °C, so the accumulative drug release is the highest when two chain segments of the copolymers exchange their hydrophobic/hydrophilic balance during the "Schizophrenic" process.

Figure 8 shows the accumulative drug release for block copolymer P(MEO_2MA-*co*-MEO_3MA)-*b*-PSPMA self-assembly aggregates at different complex stimuli conditions. There are some similarities and differences of drug release between the random and block copolymers as can be compared in Figs. 8 and 7. For P(MEO_2MA-*co*-MEO_3MA)-*b*-PSPMA self-assembly aggregates, the largest drug release amount is still under UV light irradiation at 50 °C. This result also verifies that "Schizophrenic" behaviors of self-assembly

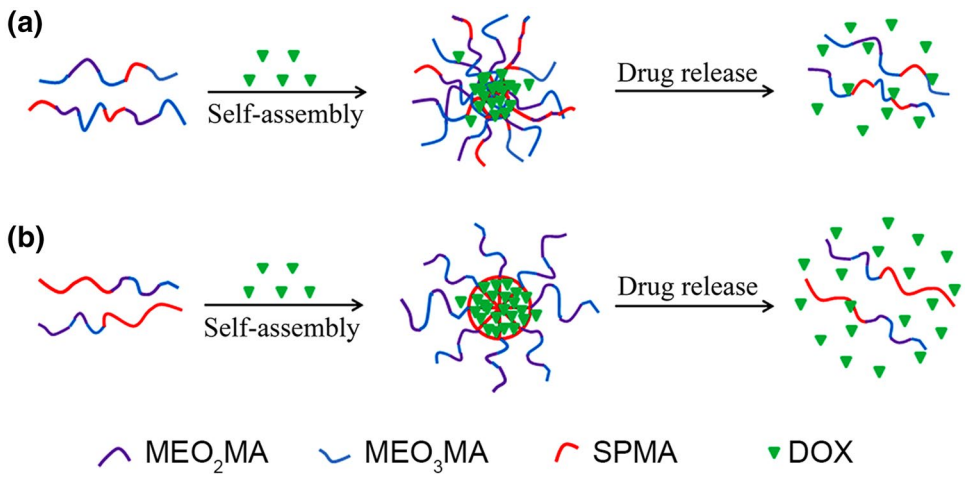

Scheme 2 Schematic representation of drug loading and release of **a** random and **b** block copolymers

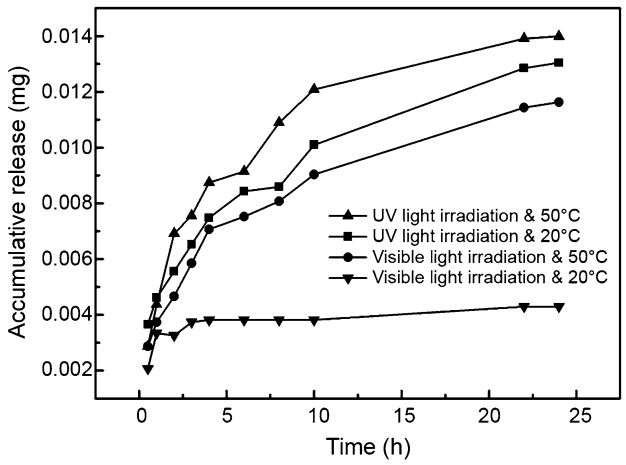

Fig. 8 Accumulative drug release for P(MEO_2MA-*co*-MEO_3MA)-*b*-PSPMA self-assembly at different stimuli conditions

allow for the highest amount of drug release. Nevertheless, the condition of the second biggest drug release amount of the block copolymer is under UV light irradiation at 20 °C, which is different from that of random copolymer shown in Fig. 7. It is due to the more regular micelle structure and morphology of block copolymer self-assembly aggregates. For the block copolymer self-assembly, a much clearer core–shell structure is formed so that it can disassemble more drugs under UV light irradiation. Since there is some drugs in the shell of self-assembly, the micelle can release a part of drugs when it is heated above its LSCT.

Conclusion

In summary, we synthesized a series of dual-responsive amphiphilic copolymers of P(MEO_2MA-*co*-MEO_3MA-*co*-SPMA) and P(MEO_2MA-*co*-MEO_3MA)-*b*-PSPMA. The structure and composition of as-synthesized copolymers were verified by ^1H NMR spectra, and their molecular weights were monitored by GPC test. Their photo-responsive property and thermo-responsive behaviors were manifested by UV–Vis absorption spectra and transmittance experiments. Critical micelle concentrations of the random and block copolymers were determined as 0.0178 mg/mL and 0.0265 mg/mL, and the micelle aggregation numbers of the random and block copolymers were calculated as approximately 17 and 13, respectively, meaning that more molecular chains were required to form stable polymeric micelle for the random than block copolymer. Specifically, the LCSTs of samples *R*4 and *X*2 were 37 °C, the human body temperature, suggesting that they might have potential application in the biomedical field. During the self-assembly process, we found the same "Schizophrenic" behaviors of copolymer self-assembly under the condition of UV light irradiation and at 50 °C. With DOX as model drug in drug release control, the results showed that heating and ultraviolet light irradiation could accelerate drug release process to some extent. All these conclusions implied that these responsive random and block copolymers might have great potential applications in drug delivery and bioengineering.

Acknowledgements This work was financially supported by the National Natural Science Foundation of China (Grant no. 21376271), the Hunan Provincial Science and Technology Plan Project, China (no. 2016TP1007), and the Undergraduates Innovative Training Foundation of Central South University (201810533294, 201810533078).

Compliance with ethical standards

Conflict of interest The authors declare no conflict interest.

References

1. Sang G, Bardajee GR, Mirshokraie A, Didehban K (2018) A thermo/pH/magnetic-responsive nanogel based on sodium alginate by modifying magnetic graphene oxide: preparation, characterization, and drug delivery. Iran Polym J 27:137–144
2. Zhang XM, Xu L, Wei SC, Zhai ML, Li JQ (2013) Stimuli responsive deswelling of radiation synthesized collagen hydrogel in simulated physiological environment. J Biomed Mater Res A 101:2191–2201
3. Farshforoush P, Ghanbarzadeh S, Goganian AM, Hamishehkar H (2017) Novel metronidazole-loaded hydrogel as a gastroretentive drug delivery system. Iran Polym J 26:895–901
4. Yan X, Wang F, Zheng B, Huang F (2012) Stimuli-responsive supramolecular polymeric materials. Chem Soc Rev 41:6042–6065
5. Dong J, Wang Y, Zhang J, Zhan X, Zhu S, Yang H, Wang G (2012) Multiple stimuli-responsive polymeric micelles for controlled release. Soft Matter 9:370–373
6. Pasparakis G, Vamvakaki M (2011) Multiresponsive polymers: nano-sized assemblies, stimuli-sensitive gels and smart surfaces. Polym Chem 2:1234–1248
7. Stuart MAC, Huck WTS, Genzer J, Müller M, Ober C, Stamm M, Sukhorukov GB, Szleifer I, Tsukruk V, Urban M (2010) Emerging applications of stimuli-responsive polymer materials. Nat Mater 9:101–113
8. Li L, Raghupathi K, Song C, Prasad P, Thayumanavan S (2014) Self-assembly of random copolymers. Chem Commun 50:13417–13432
9. Dan K, Bose N, Ghosh S (2011) Vesicular assembly and thermo-responsive vesicle-to-micelle transition from an amphiphilic random copolymer. Chem Commun 47:12491–12493
10. Yao ZL, Tam KC (2012) Temperature induced micellization and aggregation of biocompatible poly(oligo(ethylene glycol) methyl ether methacrylate) block copolymer analogs in aqueous solutions. Polymer 53:3446–3453
11. Lutz JF (2011) Thermo-switchable materials prepared using the OEGMA-platform. Adv Mater 23:2237–2243
12. Li YW, Zheng XW, Wu K, Lu MG (2016) Synthesis and self-assembly of a dual thermal and pH-responsive ternary graft copolymer for sustained release drug delivery. RSC Adv 6:2571–2581

13. Guo J, Yang W, Deng Y, Wang C, Fu S (2005) Organic-dye-coupled magnetic nanoparticles encaged inside thermoresponsive PNIPAM microcapsules. Small 1:737–743
14. Hellweg T, Dewhurst CD, Eimer W, Kratz K (2004) PNIPAM-*co*-polystyrene core-shell microgels: structure, swelling behavior, and crystallization. Langmuir 20:4330–4335
15. You YZ, Kalebaila KK, Brock SL, Oupický D (2008) Temperature-controlled uptake and release in PNIPAM-modified porous silica nanoparticles. Chem Mater 20:3354–3359
16. Tang Y, Liu L, Wu J, Duan J (2013) Synthesis and self-assembly of thermo/pH-responsive double hydrophilic brush-coil copolymer with poly(L-glutamic acid) side chains. J Colloid Interface Sci 397:24–31
17. Lutz JF, Akdemir O, Hoth A (2006) Point by point comparison of two thermosensitive polymers exhibiting a similar LCST: is the age of poly(NIPAM) over? J Am Chem Soc 128:13046–13047
18. Lutz J, Hoth A, Schade K (2009) Design of oligo(ethylene glycol)-based thermoresponsive polymers: an optimization study. Des Monomers Polym 12:343–353
19. Lutz JF (2008) Polymerization of oligo(ethylene glycol) (meth) acrylates: toward new generations of smart biocompatible materials. J Polym Sci A Pol Chem 46:3459–3470
20. Skandalis A, Pispas S (2017) PDMAEMA-*b*-PLMA-*b*-POEGMA triblock terpolymers via RAFT polymerization and their self-assembly in aqueous solutions. Polym Chem 8:4538–4547
21. Abdollahi A, Mahdavian AR, Salehi-mobarakeh H (2015) Preparation of stimuli-responsive functionalized latex nanoparticles: the effect of spiropyran concentration on size and photochromic properties. Langmuir 31:10672–10682
22. Abdollahi A, Rad JK, Mahdavian AR (2016) Stimuli-responsive cellulose modified by epoxy-functionalized polymer nanoparticles with photochromic and solvatochromic properties. Carbohydr Polym 150:131–138
23. Abdollahi A, Alinejad Z, Mahdavian AR (2017) Facile and fast photosensing of polarity by stimuli-responsive materials based on spiropyran for reusable sensors: a physico-chemical study on the interactions. J Mater Chem C 5:6588–6600
24. Mei X, Yang S, Chen D, Li N, Li H, Xu Q, Ge J, Lu J (2012) Light-triggered reversible assemblies of azobenzene-containing amphiphilic copolymer with β-cyclodextrin-modified hollow mesoporous silica nanoparticles for controlled drug release. Chem Commun 48:10010–10012
25. Rad JK, Mahdavian AR, Salehi-Mobarakeh H, Abdollahi A (2016) FRET phenomenon in photoreversible dual-color fluorescent polymeric nanoparticles based on azocarbazole/spiropyran derivatives. Macromolecules 49:141–152
26. Chen S, Liu H, Hu J, Zou H, He Y (2016) Self-assembly and morphology transition of amphipathic spiropyran-based random copolymers to control drug release. Des Monomers Polym 19:730–739
27. Abdollahi A, Mouraki A, Sharifian MH, Mahdavian AR (2018) Photochromic properties of stimuli-responsive cellulosic papers modified by spiropyran-acrylic copolymer in reusable pH-sensors. Carbohydr Polym 200:583–594
28. Paramonov SV, Lokshin V, Fedorova OA (2011) Spiropyran, chromene or spirooxazine ligands: insights into mutual relations between complexing and photochromic properties. J Photochem Photobiol C 12:209–236
29. Barrez E, Laurent G, Pavageau C, Sliwa M, Metivier R (2018) Comparative photophysical investigation of doubly-emissive photochromic-fluorescent diarylethenes. Phys Chem Chem Phys 20:2470–2479
30. Lenoble C, Becker RS (1986) Photophysics, photochemistry, and kinetics of photochromic fulgides. J Photochem 33:187–197
31. Ueki T, Nakamura Y, Lodge TP, Watanabe M (2012) Light-controlled reversible micellization of a diblock copolymer in an ionic liquid. Macromolecules 45:7566–7573
32. Rad JK, Mahdavian AR, Khoei S, Esfahani AJ (2016) FRET-based acrylic nanoparticles with dual-color photoswitchable properties in DU145 human prostate cancer cell line labeling. Polymer 98:263–269
33. Rad JK, Mahdavian AR, Khoei S, Shirvalilou S (2018) Enhanced photogeneration of reactive oxygen species and targeted photothermal therapy of C6 glioma brain cancer cells by folate-conjugated gold-photoactive polymer nanoparticles. ACS Appl Mater Interfaces 10:19483–19493
34. Lee SY, Lee H, In I, Park SY (2014) pH/redox/photo responsive polymeric micelle via boronate ester and disulfide bonds with spiropyran-based photochromic polymer for cell imaging and anticancer drug delivery. Eur Polym J 57:1–10
35. Cui H, Liu H, Chen S, Wang R (2015) Synthesis of amphiphilic spiropyran-based random copolymer by atom transfer radical polymerization for Co^{2+} recognition. Dyes Pigments 115:50–57
36. Son S, Shin E, Kim BS (2014) Light-responsive micelles of spiropyran initiated hyperbranched polyglycerol for smart drug delivery. Biomacromolecules 15:628–634
37. Barman S, Das J, Biswas S, Maiti TK, Singh NDP (2017) A spiropyran–coumarin platform: an environment sensitive photoresponsive drug delivery system for efficient cancer therapy. J Mater Chem B 5:3940–3944
38. Chen S, Gao YJ, Cao ZQ, Wu B, Wang L, Wang H, Dang ZM, Wang GJ (2016) Nanocomposites of spiropyran-functionalized polymers and upconversion nanoparticles for controlled release stimulated by near-infrared light and pH. Macromolecules 49:7490–7496
39. Zou H, Liu H (2017) Synthesis of thermal and photo dual-responsive amphiphilic random copolymer via atom transfer radical polymerization and its control release of doxorubicin. Int J Polym Mater 66:955–962
40. Liu H, Hu J, Yang X, Chen S, Cui H (2016) Preparation and characterization of dual-responsive spiropyran-based random copolymer brushes via surface-initiated atom transfer radical polymerization. Des Monomers Polym 19:193–204
41. Wu W, Wang D, Lian Y (2013) Controlled release of bovine serum albumin from stimuli-sensitive silk sericin based interpenetrating polymer network hydrogels. Polym Int 62:1257–1262
42. Yamamoto S, Joanna Pietrasik A, Matyjaszewski K (2007) ATRP synthesis of thermally responsive molecular brushes from oligo(ethylene oxide) methacrylates. Macromolecules 40:9348–9353
43. Rad JK, Mahdavian AR (2016) Preparation of fast photoresponsive cellulose and kinetic study of photoisomerization. J Phys Chem C 120:9985–9991
44. Tian WG, Tian JT (2014) An insight into the solvent effect on photo-, solvato-chromism of spiropyran through the perspective of intermolecular interactions. Dyes Pigments 105:66–74
45. Liu S, Billingham NC, Armes SP (2001) A schizophrenic water-soluble diblock copolymer. Angew Chem Int Ed 40:2328–2331
46. Liu S, Armes SP (2002) Polymeric surfactants for the new millennium: a pH-responsive, zwitterionic, schizophrenic diblock copolymer. Angew Chem Int Ed 41:1413–1416
47. Zhou YN, Zhang Q, Luo ZH (2014) A light and pH dual-stimuli-responsive block copolymer synthesized by copper(0)-mediated living radical polymerization: solvatochromic, isomerization, and "schizophrenic" behaviors. Langmuir 30:1489–1499